Key Engineering Materials, "Defect and Diffusion Forum" vols. 194-199 (2001).

Atomic Transport at Liquid Metal/Al_2O_3 Interfaces

E. Saiz, R. M. Cannon and A. P. Tomsia

Materials Sciences Division

Lawrence Berkeley National Laboratory

Berkeley, CA 94720, USA

Keywords: Ceramic-Metal interfaces, Wetting, Diffusion processes, Transport mechanism, Grain boundary grooves,

Abstract In this work, atomic force microscopy (AFM) has been used to identify the controlling transport mechanisms at metal/oxide interfaces and measure the corresponding diffusivities. Interfacial transport rates in our experiments are two to four orders of magnitude faster than any previously reported rates for the oxide surface. The interfacial diffusivities and the degree of interfacial anisotropy depend on the oxygen activity of the system. Atomic transport at metal/oxide interfaces plays a defining role in many technological processes, and these experiments provide fundamental data for the formulation of the atomic theory needed to explain many of the observed phenomena.

Introduction

The atomic theory of metal/oxide interfaces is in the early stages of formulation. Two of the main problems are the inherent complexity of many of the measurable interfacial properties (such as interfacial strength or friction) and the lack of systematic experimental data that could be contrasted with the theory. Because the continuum theory of capillary-driven mass transport is well established, measurement of the morphological evolution of interfaces can provide the basic data needed for understanding the atomic structure of metal/oxide boundaries. These “mesoscopic” experiments can also provide the intermediate step needed to link the atomic theory to technological processes such as composite sintering, refractory corrosion, metal-ceramic joining, thin film stability, supported metals catalysts and liquid metal spreading.

One of the ways capillary mass transport manifests itself is by the development of a grain boundary groove on the surface of a polycrystalline material whenever a boundary intersects an interface between a solid and another phase (fluid or solid). The groove forms in order to achieve complete local equilibrium of the interfacial forces at the triple junction (groove root), and its growth results from transport of mass from the high curvature region near the root to the flatter parts of the interface. Mass transport can involve several mechanisms: interfacial diffusion, volume diffusion on either side of the interface, and interfacial reaction (solution-precipitation or evaporation-condensation if the fluid phase is liquid or gas, respectively). Depending on the physical characteristics of the system and groove size, one of these mechanisms will be rate controlling, resulting in characteristic groove shapes and growth kinetics [1-4].

Experimental

In the present work, scanning electron microscopy (SEM) and atomic force microscopy (AFM) were used to study the evolution of grain boundary grooves at the interface between liquid metals (Ni, Cu, Au, Al) and pure polycrystalline alumina (99.997%, Showa-Denko, Japan). Our main objective was to determine the operative transport mechanisms at the interfaces and the corresponding diffusivities

or solution-precipitation rates. Metal/oxide systems are in fact ternary systems where the oxygen partial pressure $p(O_2)$ is a fundamental variable. For a given metal/oxide couple, a range of $p(O_2)$ can be determined where both phases can coexist in equilibrium (no chemical reaction occurs at the interface). It is now recognized that at the high and low $p(O_2)$ limit of this coexistence range, adsorption can occur in all the three interfaces involved (the metal and oxide surfaces and the metal/oxide interface). However, for many systems there is a intermediate range of $p(O_2)$ where no adsorption takes place and all the interfaces are stoichiometric [5]. All experiments in this work have been performed in the range of oxygen partial pressures within which no chemical reactions between the metal and the oxide occur and in which no adsorption is anticipated (with the exception of Al, which is a binary system with only one oxygen partial pressure at which the metal and the oxide can coexist in equilibrium) [5].

Small pieces of the selected metals were melted in Ar ($p(O_2)$~10^{-13} Pa) on pure alumina substrates for different times. Experiments with Au were performed in air inside a closed sapphire crucible, embedded in Al_2O_3 powder. The polished alumina substrates had an average grain size of 20 μm. After firing, the metals were chemically etched, and the area under the metals was analyzed by SEM and AFM. The profiles of the boundary grooves at the solid/liquid and solid/vapor interfaces were measured using AFM line analysis in the constant-force mode. In order to study the evolution of grooves with time, pieces of the metals were consecutively melted at the same place on the substrate, and the interface was analyzed after sequential heating and etching steps. This process was repeated two to six times. Parallel studies of boundary grooving on free alumina substrates were performed at the same temperatures and atmospheres used in the metal/ceramic experiments. Al/Al_2O_3 experiments were also carried out in gettered Ar, placing an Al_2O_3 substrate in a closed alumina crucible, close to an Al drop. It is expected that, under those conditions, the $p(O_2)$ inside the crucible would be close to the phase boundary value for the Al/Al_2O_3 system.

Results and Discussion

The observed grain boundary grooves at all the solid/liquid interfaces were unexpectedly much wider than those at the solid/vapor interfaces (Figure 1). This result indicates that the mass transport involved in grooving at the metal/ceramic interfaces is orders of magnitude faster than on the free surface. In every case, the shape of the groove, recorded using AFM line profiles perpendicular to the grooves (Figure 2), shows the presence of a hump at each side, corresponding to growth controlled by a diffusion mechanism rather than by the dissolution/precipitation rates.

Transport of the Al_2O_3 involves diffusion of both Al and O ions or atoms. This diffusion could occur through the liquid metal, along the interfaces, or through the oxide itself. Based on known data for volume diffusion coefficients of alumina [6], diffusion through the oxide is too slow to be considered. Although each species could move independently along either path, the dissolution and deposition must involve stoichiometric Al_2O_3. Thus, the potential gradients for each species will be adjusted so that the sum of the departure or arrival rates from both paths are in stoichiometric proportion everywhere along the interface. Since the shape of an evolving groove is similar for either interfacial or volume controlled diffusion [1-4], the fluxes from the two paths can be combined in a simple manner to give the rate of groove growth [1-3]:

$$\frac{3w^3}{5^3}\frac{dw}{dt} = \frac{\left(2.7B_i^{Al} + wB_V^{Al}\right)\left(2.7B_i^{O} + wB_V^{O}\right)}{3\left(2.7B_i^{Al} + wB_V^{Al}\right) + 2\left(2.7B_i^{O} + wB_V^{O}\right)} \tag{1}$$

where w is the groove width, measured as the distance between the two maximums (top of the humps) in the profile at both sides of the groove. The interfacial and volume transport coefficients for each species (B_i, B_V) are:

$$B_i = \frac{\omega D_i \gamma_i \Omega}{kT} \tag{2}$$

$$B_V = \frac{x D_V \gamma_i \Omega}{kT} \tag{3}$$

Ω is the molecular volume, ω is the interfacial width, x is the molar solubility in the metal for the diffusing species, and D_i and D_v are the interfacial and volume diffusivities.

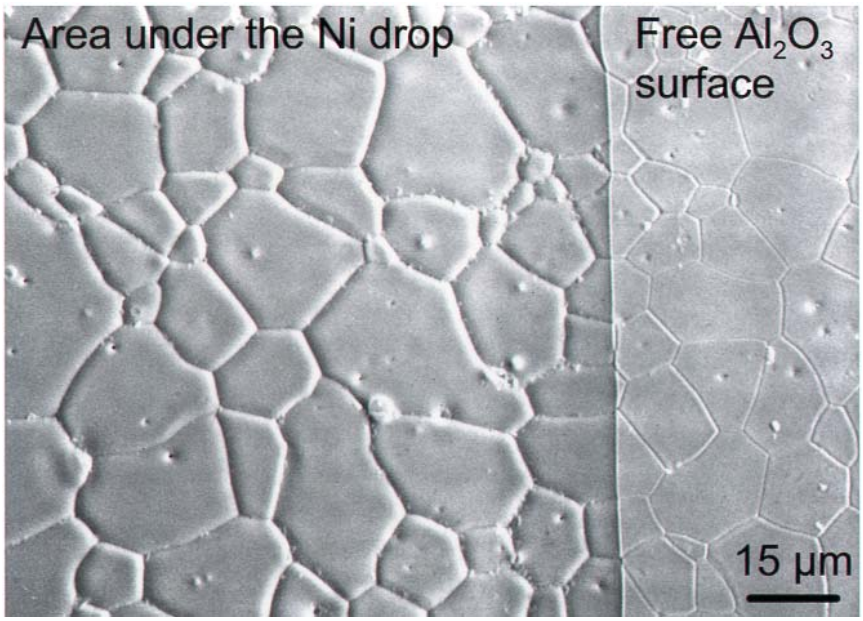

Figure 1. SEM image of an alumina substrate after removing a Ni drop (melted for 1 hour at 1773 K). Grain boundary grooving is enhanced in the area under the liquid.

This model is analogous to the ambipolar coupling expected for creep [6,7] or sintering in which transport is limited by the slower species along its fastest path. More rapid diffusion by either species over both paths would result in an additive relationship, in which the slow species would be controlling via interface transport at small grooves and volume transport would be limiting at large widths. For example, if oxygen transport were faster (as has been typically assumed for the free surface of Al_2O_3 [8]) Equation [1] reduces to:

$$\frac{3w^3}{5^3}\frac{dw}{dt} = \frac{\left(2.7B_i^{Al} + wB_V^{Al}\right)}{2} \tag{4}$$

The qualitative trends would be similar if the diffusion species were complexes, e.g. AlO_x, assuming they have different stoichiometry than Al_2O_3.

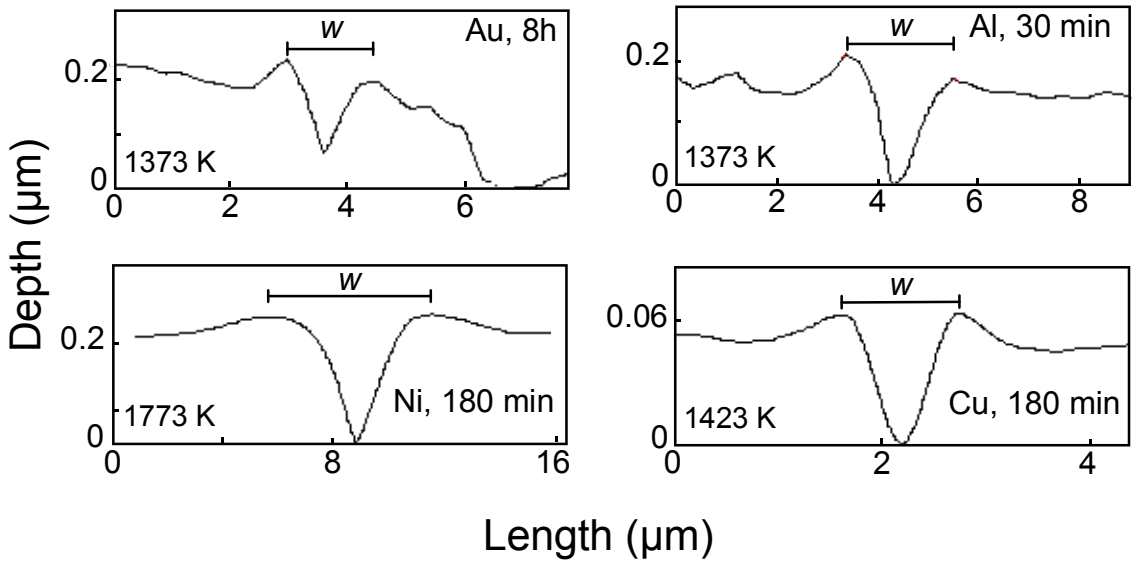

Figure 2. AFM profiles across grain boundary grooves at metal/Al_2O_3 interfaces. The groove shapes indicate that mass transport is mostly controlled by diffusion. The width of the groove (w) is measured as the distance between the maximum in the profile at each side of the groove.

Three kinds of fits have been attempted to discover which diffusion process is rate controlling:

$$w = 4.6(\frac{B_i t}{2})^{1/4} + w_0 \text{ (interfacial diffusion control)} \quad (5)$$

$$w = 5(\frac{B_V t}{2})^{1/3} + w_0 \text{ (volume diffusion control)} \quad (6)$$

$$w = 4.6(\frac{B_i t}{2})^{1/4} + 5(\frac{B_V t}{2})^{1/3} + w_0 \text{ (combined)} \quad (7)$$

where w_0 is the initial width. The evolution of the average groove widths, w, measured from 80 to 100 boundaries per sample, and the corresponding fittings are presented in Figure 3. The fitting results for all the systems are summarized in Table 3; these assumed $\Omega/2$, the volume per Al ion, is $2.12 \cdot 10^{-29}$ m^3 and γ_v values were taken from literature [5, 9-10]. When the results seemed implausible or fewer than four measurement times were available, w_0 was put at 0. The transport mechanism can be deduced, taking into account the physical implications of the calculated diffusivities and w_0 values and the comparison between the combined and single-mechanism fittings.

The surface diffusivities calculated for the alumina surfaces annealed in the same atmosphere were in the band of the reported diffusivities for pure Al_2O_3 (Figure 4) and, with the exception of Al, did not depend on the presence of a metal drop on the substrate. This agrees with the hypothesis that for all the other metals the experiments were carried at oxygen partial pressures were no adsorption occurs on any of the interfaces.

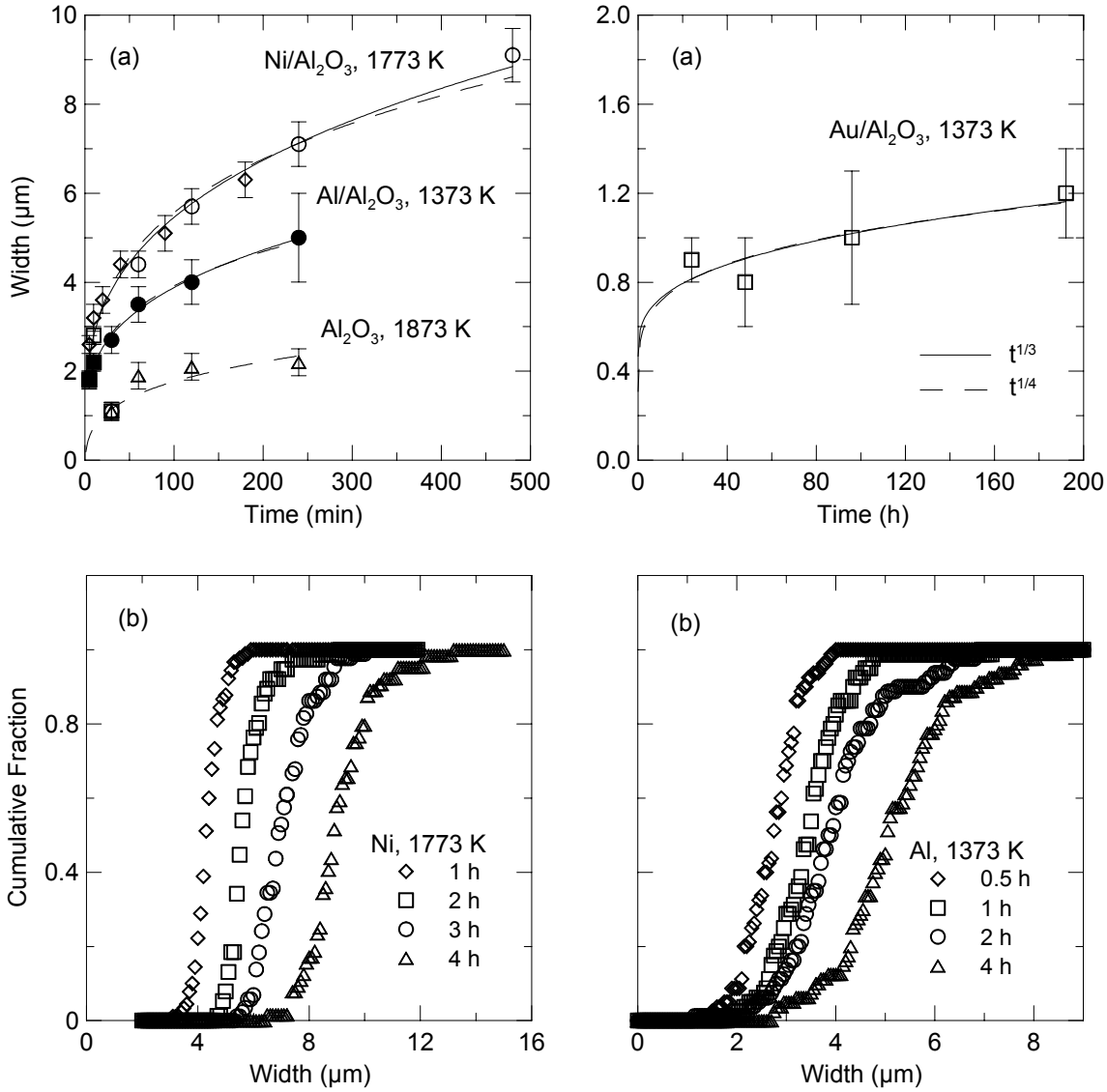

Figure 3. (a) Time evolution of average groove widths at the surface of alumina and metal/Al_2O_3 interfaces. Fitting to $t^{1/3}$ (volume diffusion) and $t^{1/4}$ (surface diffusion) laws is shown. (b) Statistics of groove widths measured after different times on Al and Ni interfaces with the same Al_2O_3 substrates.

For the Ni/Al_2O_3 interface, fitting to an interfacial diffusion controlled process (Equation 5) was unsatisfactory because the calculated initial groove thickness (w_0) being negative is unrealistic. In addition, the calculated interfacial diffusivities are two to four orders of magnitude larger than those measured on the surface of alumina. On the other hand, the volume diffusivities calculated from the combined and $t^{1/3}$ fittings are very similar, leading to the conclusion that, for the groove widths measured in this work, the rate controlling mechanism is volume diffusion. The result of the $t^{1/4}$ fitting represents an upper limit for the possible contribution of interfacial diffusion, with the value calculated from the combined fitting being closer to the real one. Although Equation (7) is only an approximate solution to Equation (4), extremely large errors result from fitting to the exact solution (3) because of its mathematical form. The value of ωD_i from Equation (7) may be representative of interface diffusion for stoichiometric interfaces and is in the range of values reported for the surface diffusion of alumina (Figure 4). If volume diffusion is the controlling mechanism, it has to be diffusion through the liquid. The Al self-diffusion coefficients in Al_2O_3 are more than 3 orders of

magnitude smaller than those required (Table 1) and those for O are even smaller [6]. It is recognized that dissolved NiO and FeO are reported to enhance creep of Al_2O_3 under conditions considered to be controlled by lattice diffusion [6,7]; but at the low $p(O_2)$ values used here, the solubility is deemed to be too low to sufficiently influence the Al_2O_3 defect concentrations.

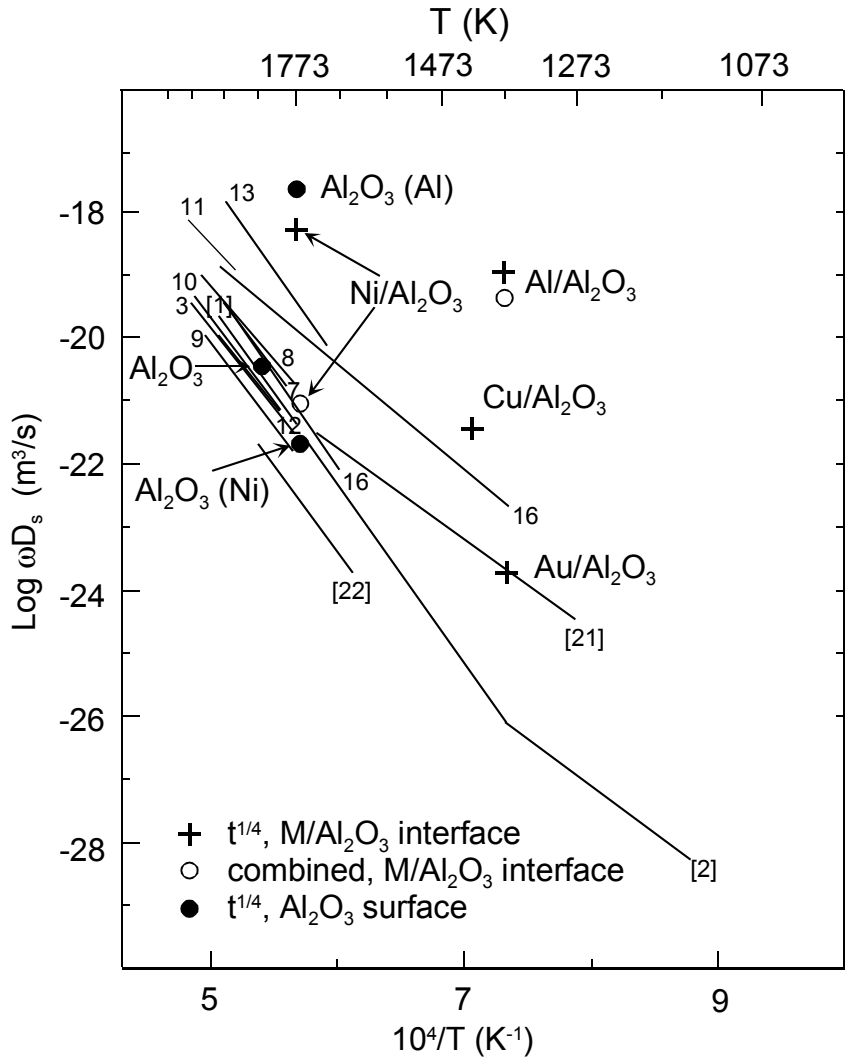

Figure 4. Calculated interfacial diffusivities for metal/alumina systems compared with those reported by others for the alumina surface. For metal/alumina interfaces, the crosses correspond to an upper limit, calculated assuming the $t^{1/4}$ fitting; the open circles correspond to results obtained from the combined fitting. Unbracketed numbers are references in ref. [8].

Because of small groove dimensions, the errors in the measurements of grooves at the Cu and Au/Al_2O_3 interfaces preclude the combined fitting. In the gold system, the grooves are visible at the interface but not at the oxide surface for samples annealed in air and not after Ar anneals. The $t^{1/4}$ fitting for the air annealed samples yields Au/Al_2O_3 interfacial diffusivities like those measured on the surface of impure Al_2O_3 and over two orders of magnitude higher than those on pure alumina. At a similar temperature, the upper-bound interfacial diffusivity calculated for the Cu interface using Equation (5) is two orders of magnitude higher. Since a physical mechanism that could explain such a big difference in interfacial diffusivities at similar temperatures has not been formulated, the results suggest that grooving at the Cu/Al_2O_3 interface is controlled by volume diffusion.

Table 1
Calculated Surface and Volume Diffusivities

System	Temp (K)	Surface Diffusion		Volume Diffusion		Combined		
		$\omega \cdot D_i$ ($m^3 \cdot s$)	w_0 (nm)	$x \cdot D_v$ ($m^2 \cdot s$)	w_0 (nm)	$\omega \cdot D_i$ ($m^3 \cdot s$)	$x \cdot D_v$ ($m^2 \cdot s$)	w_0 (nm)
Al_2O_3	1873	$4.6 \cdot 10^{-21}$	0					
Al_2O_3 (Ni)	1773	$2.0 \cdot 10^{-22}$	0					
Al_2O_3 (Al)	1773	$2.6 \cdot 10^{-18}$	2688					
Ni/Al_2O_3	1773	$4.4 \cdot 10^{-19}$	-795	$1.1 \cdot 10^{-13}$	525	$8.4 \cdot 10^{-22}$	$5.9 \cdot 10^{-14}$	220
Au/Al_2O_3	1373	$1.8 \cdot 10^{-24}$	195	$3.5 \cdot 10^{-18}$	385			
Cu/Al_2O_3	1423	$2.8 \cdot 10^{-22}$	0	$7.8 \cdot 10^{-16}$	0			
Al/Al_2O_3	1373	$1.1 \cdot 10^{-19}$	-162	$5 \cdot 10^{-14}$	630	$4.1 \cdot 10^{-20}$	$6.6 \cdot 10^{-16}$	0

If the relevant transport mechanism were volume diffusion, some $p(O_2)$ dependence would be expected. In this case, the diffusion of the species (Al, O, or some complexes of them) with the lower xD_V product will control grooving kinetics. Since, in the presence of Al_2O_3 aluminum and oxygen solubilities are related, $a_{Al}^2 a_O^3 = K(T)$, the grooving kinetics are expected to vary continuously with oxygen partial pressure. In that case, diffusion of Al would be limiting at higher $p(O_2)$, whereas diffusion of O would be limiting at very low $p(O_2)$. Assuming that the volume diffusion coefficient is $D_V \approx 10^{-9}$ $m^2 \cdot s^{-1}$ (a typical value for liquid metals [11], the estimated solubility of the slow species in Ni is $\sim 10^{-4} - 10^{-5}$. This seems plausible compared to measurements of Al or O solubility in liquid Fe [12] and solid Ni [13] in equilibrium with Al_2O_3.

However, the nonlinear activity coefficients indicate that the dissolved species are highly associated, which blocks making quantitative extrapolations to the low $p(O_2)$ values. For Cu, the implied solubility is $\sim 10^{-6}$, much lower than in Ni, despite the solubilites for O being similar in the two metals at higher $p(O_2)$. In the Au/Al_2O_3 system annealed in gettered Ar, grooving was much slower than in air (no groove appeared even after 24 hours at 1373 K). The results suggest a strong dependence on $p(O_2)$ that would imply a volume diffusion hypothesis, but, surprisingly, with O being the slower species even at high $p(O_2)$. The solubilities would again be some orders of magnitude lower in the Au than in Cu (obviously, further work is necessary to clarify these points).

The interfacial diffusivities should not depend on the oxygen partial pressure when there is no adsorption, but with oxygen or aluminum adsorption, some variation could be expected. Because, Al and O activities are related, reducing the activity of oxygen increases the activity of Al in the liquid. For many metal-aluminum systems, all the compositions of the binary system are molten at temperatures just above the melting point of the metal M, resulting in a fully miscible liquid metal phase. Then, the composition of the liquid in equilibrium with alumina is nearly pure Al at the low $p(O_2)$ phase boundary and increases rapidly in its M content with rising oxygen activity; it becomes nearly pure M after a few orders of magnitude increase in $p(O_2)$ [5]. Thus, study of the Al/Al_2O_3 interface should reveal trends expected at very low oxygen activity. The shapes of the grain boundary grooves formed at 1373 K on the Al/Al_2O_3 interface correspond to diffusion-controlled growth, albeit perturbed by faceting. However, mass transport is several orders of magnitude faster than at or near the Au or Cu/Al_2O_3 interfaces at similar temperatures.

Comparison of the $t^{1/3}$, $t^{1/4}$ and combined fittings (Table 1) suggests that the transport is primarily at the interface, but the data are not good enough to eliminate the possibility of volume diffusion from making a large or even dominant contribution to groove growth. The estimated solubility of O in Al from very limited data, $\sim 8 \cdot 10^{-6}$ [14], is consistent with transport along both paths and less than implied for transport exclusively through the liquid. Most strikingly, however, the upper limit for the interfacial diffusivity ($t^{1/4}$ fitting) and the value from the combined equation are similar and far larger than ever reported for any alumina surfaces (Figure 4) [8] True, most of the values reported for alumina have been from experiments performed at oxygen pressures far larger than the one at which aluminum and alumina coexist in equilibrium. Even so, the interfacial diffusivities should not depend on the oxygen partial pressure when there is no adsorption; some variation could be expected with oxygen or aluminum adsorption. The relevant interface diffusivity here would likely be that for O instead of Al, and is for an Al-rich interface.

In experiments to investigate the effect of low $p(O_2)$ on the surface diffusion of pure alumina we made an important discovery. The calculated surface diffusivity (Figure 4) is orders of magnitude greater than any observed before [8] These experiments were carried out in gettered Ar, with an Al_2O_3 substrate in a closed alumina crucible close to an Al drop. Most of the boundary grooves that formed on the alumina have a shape expected for a diffusion-controlled process (although faceting altered the shape of some). Note that the previous reported data for the surface diffusivity of alumina has been taken at much higher $p(O_2)$. Although vapor transport may be suspected, the implied $t^{1/2}$ fit was unsatisfactory. This result underlines the often neglected effect of oxygen activity on the oxide surface properties.

Both the surface anisotropy and interfacial transport rates depend on environment in a manner that depends in part on $p(O_2)$. The interfacial diffusion at the Al/Al_2O_3 interface and the surface diffusion of alumina at the corresponding equilibrium $p(O_2)$ are much higher than the values measured for the stoichiometric surface. This difference may be consistent with there being an excess of Al at both the surfaces and interfaces.

Another important and unexpected difference between the Al/Al_2O_3 and the stoichiometric interfaces is that the former appear to be much more anisotropic (Figures 5 and 6). The Al/Al_2O_3 interfaces are strongly faceted, and the hexagonal shape of some facets (Figure 5b) suggests that the alumina basal plane is a low energy surface when in contact with Al. In contrast, the interfaces with Ni appear to be very nearly isotropic, with smooth and rounded shapes and only few visible facets, more so than the free surface of alumina seen here (Figures 5 and 6) and elsewhere [15,16]. This anisotropy also results in wider distributions of groove widths (Figure 3) for the Al/Al_2O_3 interface. The Al_2O_3 surfaces outside the Al drops seem to be less strongly faceted than those under Al, but somewhat more so than the stoichiometric surfaces of Al_2O_3. The enhanced faceting is in part a result of more rapid transport, but the basal plane has clearly become relatively more stable for the interface and seemingly also for the surface.

The effect of oxygen activity on the interfacial anisotropy has not been systematically studied. These results indicate a change in the Wulff plot for the sapphire-vapor surface versus those recently reported [17,18] for higher oxygen activities and would be consistent with the idea that the surfaces oriented parallel to alternating sheets of O and Al atoms in the crystal structure may be partially reduced more readily. The (0001) plane has been shown to become Al rich in UHV [19,20]. Evidently, the situation is analogous for the liquid Al/Al_2O_3 interface.

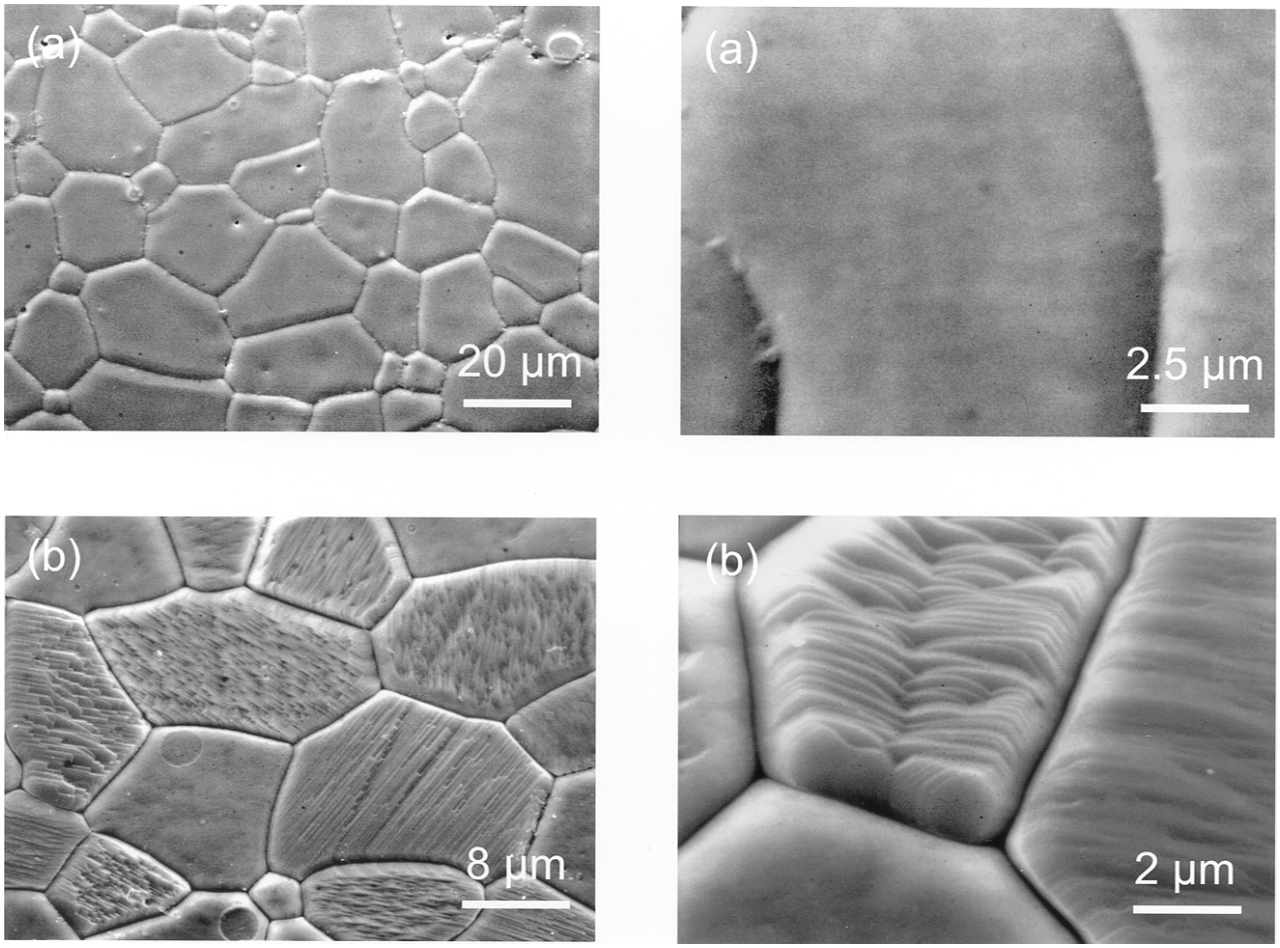

Figure 5. SEM images of the surfaces of alumina substrates: (a) after removing a Ni drop (melted 1 hour at 1773 K), (b) free surface (annealed for 5 hours at 1973 K in gettered Ar) and (c) after removing an Al drop (melted 30 min at 1373 K).

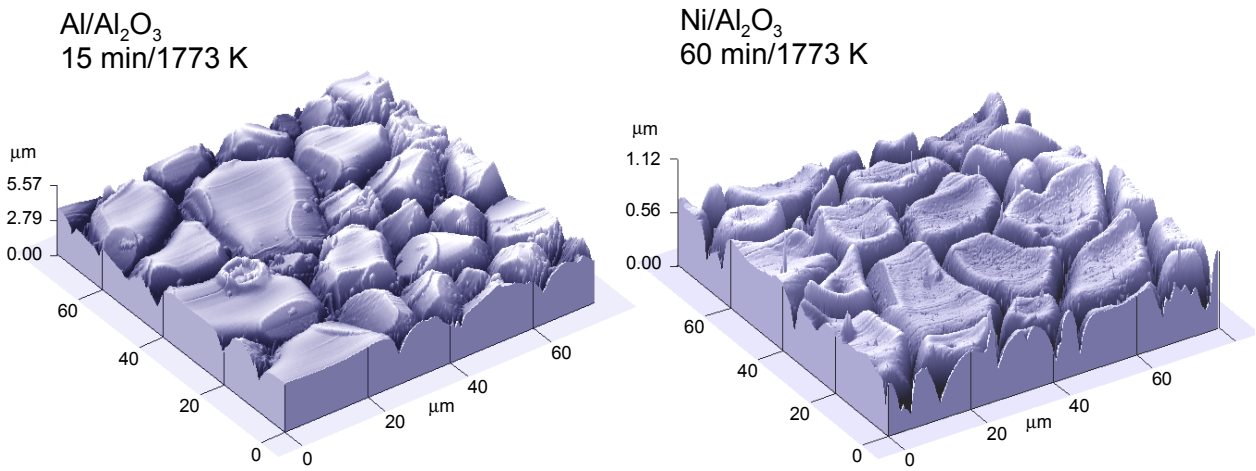

Figure 6. AFM images of alumina substrates after removing Ni (melted 1 hour at 1773 K) and Al (melted 15 minutes at 1773 K).

Conclusions

The results presented here provide fundamental data necessary for the modeling of those technological processes that involve the interaction between liquid metals and oxides. These results also provide data needed for the development of an atomic theory of kinetic processes at metal/ceramic interfaces. Such a theory should provide a basis for understanding the relation between the diffusivities at the metal/ceramic interfaces and the oxide surface. It should account for the observed fast transport rates near the metal/oxide interface and the observed increase in transport rates when decreasing the oxygen activity in the system. It should also explain the observed transition from the isotropic stoichiometric interfaces to the anisotropic ones observed at very low oxygen activity, when adsorption is expected to occur.

Acknowledgments. Work supported by Director, Office of Energy Research of U.S. Department of Energy under contract No. DE-AC03-76SF00098.

References

[1] W. W. Mullins, *J. Appl. Phys.*, **28**, 1957, 333.

[2] W. W. Mullins, *Trans. Met. Soc. AIME*, **218**, 1960, 354.

[3] W. W. Mullins and P. G. Shewmon, *Acta Metall.*, **7**, 1959, 163.

[4] W. M. Roberston, *J. Appl. Phys.*, **42**, 1971, 463.

[5] E. Saiz, A. P. Tomsia, R. M. Cannon in *Ceramic Microstructures: Control at the Atomic Level*, A. P. Tomsia and A. M. Glaeser, Ed., Plenum Press, N. Y.,1998, 65.

[6] R. M. Cannon and R. L. Coble, *Deformation of Ceramic Materials*, ed R. C. Bradt and R. E. Tressler, Plenum Press, N. Y., 1975, 61.

[7] R. S. Gordon, *J. Am. Ceram. Soc.*, **56**, 1973, 147.

[8] J. M. Dynys, R. L. Coble, W. S. Coblenz and R. M. Cannon, *Sintering Processes*, ed. G. C. Kuczynski, Plenum Publishing Corporation, 1980, 391.

[8] K. Nogi, K. Oishi, K. Ogino, *Mater. Trans., JIM*, **30**, 1989, 137.

[10] B. J. Keene, *Inter. Mat. Rev.*, **38**, 1993, 157.

[11] C. J. Smithells, Ed., *Metals Reference Book*, (Butterworths, London & Boston, 1976) pp. 939.

[12]. R. Holcomb and G. R. St. Pierre, *Metall Trans B*, **23B**, 1992, 789.

[13] K. P. Trumble and M. Rühle, *Acta Metall. Mater*., **39**, 1991, 1915.

[14] H. A. Wriedt, *Bull. Alloy Ph. Diag.*, **6**, 1985, 548.

[15] C. A. Handwerker, J. M. Dynys, R. M. Cannon and R. L. Coble, *J. Am. Ceram. Soc.*, **73**, 1990, 1365.

[16] C. A. Handwerker, J. M. Dynys, R. M. Cannon and R. L. Coble, ibid., 1371.

[17] J.–H. Choi, D.–Y. Kim, B. J. Hockey, S. M. Wiederhorn, C. A. Handwerker, J. E. Blendell, W. C. Carter, A. R. Roosen, *J. Am. Ceram. Soc.*, **80**, 1997, 62.

[18] M. Kitayama, and A. M. Glaeser, *Key Eng. Mater*., **159-160**, 1998, 193.

[19] T. M. French and G. A. Somorjai, *J. Phys. Chem*., **74**, 1970, 2489.

[20] M. Gautier, G. Renaud, L. P. Van, B. Villette, M. Pollak, N. Thromat, F. Jollet, J. –P. Duraud, *J. Am. Ceram. Soc*., **77,** 1994, 323.

[21] A. Tsoga and P. Nikolopoulos, *J. Am. Ceram. Soc.*, **77**,1994, 954.

[22] W. Shin, W.–S. Seo and K. Koumoto, *J. Eur. Ceram. Soc.*, **18**, 1998, 595.